

Design and Implementation of a Very Compact MIMO Antenna Providing Dual Notches at WLAN and X-Band

Guvvala Ramya Sri, Areti Jhansi Rani, and Vanka Saritha*

Abstract—A very compact Multiple-Input-Multiple-Output (MIMO) radiator providing dual notches is presented in this paper. It comprises circular ring monopoles fed by a microstrip line embedded with a slot of inverted U-shape. By etching a crescent slot, a split ring resonator slot, a circular slot in the circular monopole, a reversed U-shaped slot inserted along the feeding line, two notches are attained. It operates from 3.5 GHz to 12 GHz that overcomes interference from the Wireless Local Area Network (WLAN) (5.15–5.85 GHz) and X-band (7–8.1 GHz). MIMO antenna has a very compacted dimension of $44\text{ mm} \times 44\text{ mm} \times 1.6\text{ mm}$ at the lowest operating frequency and hence is suitable for portable devices. It has dimensions of $0.51\lambda \times 0.51\lambda \times 0.018\lambda$ where λ is the wavelength of the lowest operating frequency 3.5 GHz.

1. INTRODUCTION

Ultra Wide Band (UWB) communication is usually accomplished by means of either the preferred technology that is radio based UWB abbreviated as IR-UWB, or UWB based on Orthogonal Frequency Division Multiplexing abbreviated as UWB-OFDM. IR based UWB is implemented by the transmission of extraordinarily short pulses, while in OFDM-based UWB, orthogonal subcarriers exist to adjust the data that are transmitted [1]. As per the Federal Communications Commission (FCC), UWB systems remain permitted to operate from 3.1 to 10.6 GHz devoid of an exemption obligation for commercial applications [2]. UWB technologies are in great demand due to its numerous advantages i.e., high data rate, performance of robust anti-interference, low consumption of power, good suppression, huge capacity for communication, and less cost [3].

A compact MIMO antenna with high isolation is used to improve impedance matching and to obtain a notched band at WLAN, i.e., 5.15–5.85 GHz & Super-Extended C-band, i.e., from 6.7–7.1 GHz [4]. A MIMO antenna with coplanar waveguide feed is proposed aiming at the notched bands viz WLAN and global system for mobile communications. Novelty of the antenna design is that it does not involve any added circuit elements for attaining extraordinary isolation level and to obtain notches at 4.8 and 7.7 GHz [5].

A scheme to diminish mutual coupling between the elements by modifying the dimension of a cup-shaped branch and SIR structure to attain the dual notches at WLAN & X-band is presented [6]. A four-port polarization diversity antenna which exhibits large operating bandwidth suitable for attaining extraordinary data rate and diverse techniques that help in notches filtering at 3.5 GHz and 5.5 GHz bands are achieved [7]. Stepped ground plane is employed to increase the impedance bandwidth. The interference intended for Worldwide-Interoperability -for- Microwave-Access (WiMAX) and WLAN bands is rejected by means of U-shaped slots, in the radiating plane and dual L-shaped slots that are of quarter wavelength in the stepped ground plane [8]. A four-port MIMO antenna with a metal strip

Received 27 June 2020, Accepted 6 August 2020, Scheduled 20 August 2020

* Corresponding author: Vanka Saritha (vankasaritha2@gmail.com).

The authors are with the Department of Electronics & Communication Engineering, V R Siddhartha Engineering College, A. P., India.

of + shape inserted into the ground of the antenna decreased coupling amongst the radiators and also obtained narrow notched bands at 3.5 GHz corresponding to Wi-MAX and at 5.5 GHz corresponding to WLAN [9]. A compact antenna that has four feeding ports with effective radiation characteristics, stable gain, and acceptable envelope correlation coefficient is proposed. Split-ring resonator slots are etched on the patch, with two rhombic-shaped monopoles orthogonal to each other which improve the performance regarding envelope correlation coefficient and diversity gain. This design obtains the dual band notches at Wi-MAX & WLAN bands [10]. In all the designs discussed above, some designs use two-port MIMO; some designs reject WLAN and C bands, WiMAX and WLAN, and rejection of broad bands is observed. There exist antennas that reject WLAN and X-band, but extra bands of frequencies other than desired WLAN and X-bands are also rejected. The proposed design aims at a compact design with four-port MIMO that can reject intended WLAN and X-band satellite communication link.

This paper proposes a MIMO antenna with dual notches at WLAN and X-bands. A single element is a circular monopole fed by a microstrip line. It has a ground plane that is defected with a semicircle slot etched in the middle. A circular monopole element is used, and a crescent ring resonator is inserted on it, by using a rectangular spiral slot carved in the feed line in order to attain the refusal of bands at WLAN (5.15–5.85 GHz). Further when the U-shaped slot along with a circular slot is etched on the circular monopole antenna, band rejection is obtained at X-band (7–8.15 GHz). The antenna operates from 3.5 to 12 GHz, with band rejections at WLAN and X-bands. The antenna is simulated using HFSS, and its parameters of reflection coefficient, voltage-standing-wave-ratio (VSWR), gain, radiation pattern, correlation coefficient of envelope, total active reflection coefficient, and diversity gain are plotted.

2. EVOLUTION OF PROPOSED ANTENNA DESIGN

The schematic of the single element design is depicted with dimensional details as shown in Figure 1. It is a microstrip fed monopole printed antenna. The printed antenna comprises an ARLON (AD430) substrate with a relative dielectric-constant of 4.3, i.e., ϵ_r , thickness of 1.6 mm having loss tangent of 0.02. The electromagnetic simulations are carried out by means of HFSS (High-Frequency-Structure-Simulator). The dimensions are presented in Table 1.

Table 1. Dimensions of single element.

| Antenna parameter | Value (mm) | Antenna parameter | Value (mm) | Antenna parameter | Value (mm) |
|-------------------|------------|-------------------|------------|-------------------|---------------------|
| L | 23.3 | $W1$ | 3 | $R6$ | 1.4 |
| $L1$ | 8 | $W2$ | 4.9 | $t1$ | 1.5 |
| $L2$ | 3 | $R1$ | 6.8 | $t2$ | 1.25 |
| $L3$ | 8.5 | $R2$ | 5.8 | $O1$ | 12.2 (from the top) |
| $L4$ | 5.6 | $R3$ | 5.2 | $O2$ | 12.5 (from the top) |
| $r1$ | 2.75 | $R4$ | 3.4 | $O3$ | 14.3 (from the top) |
| W | 14.5 | $R5$ | 2.4 | $h1$ | 3.4 |

Stages of Evolution: Peculiar stages are involved in the evolution of proposed element in obtaining dual band notches in the operating wide band which are shown in Figure 2.

Stage-1: It comprises a circular monopole that is fed by means of a microstrip line with an impedance transformer at the joining of the antenna and the feed line. It has a defected ground structure of rectangular shape. The antenna operates from 3.5 to 12 GHz.

Stage-2: It comprises a circular monopole that is fed by means of a microstrip line with an impedance transformer at the joining of the antenna and the feed line. As a way to improve the impedance bandwidth, the defected ground structure is etched with a semicircle etched in it at its center. The antenna operates from 3.5–12 GHz.

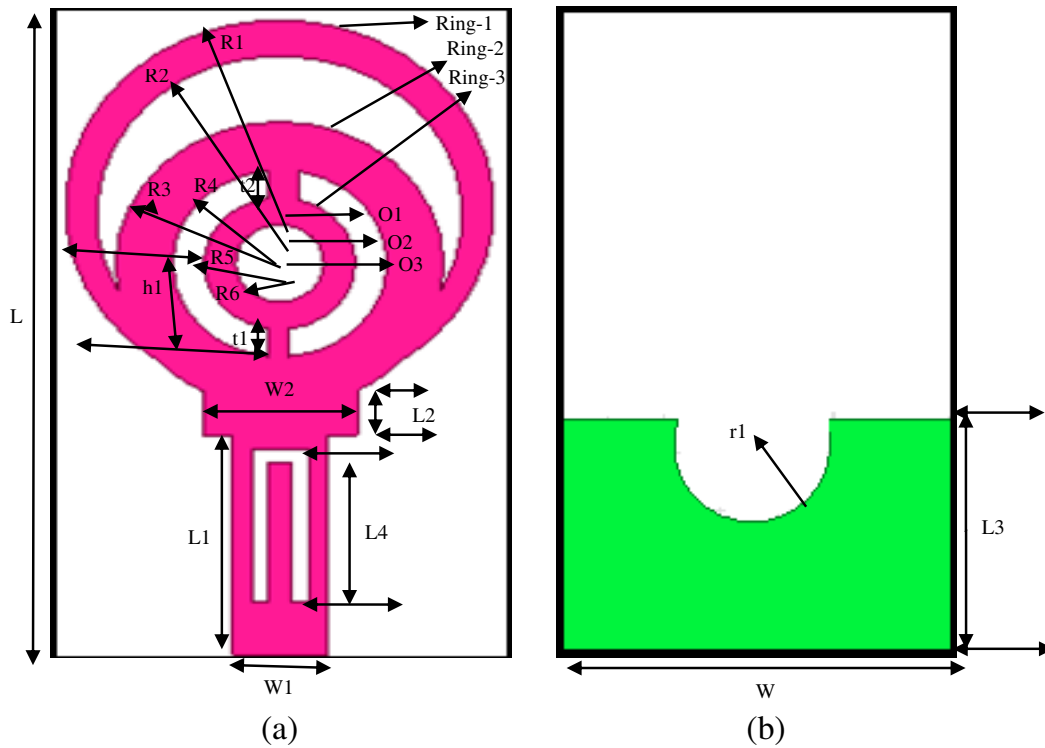


Figure 1. Geometry of the single element: (a) top vision and (b) bottom vision.

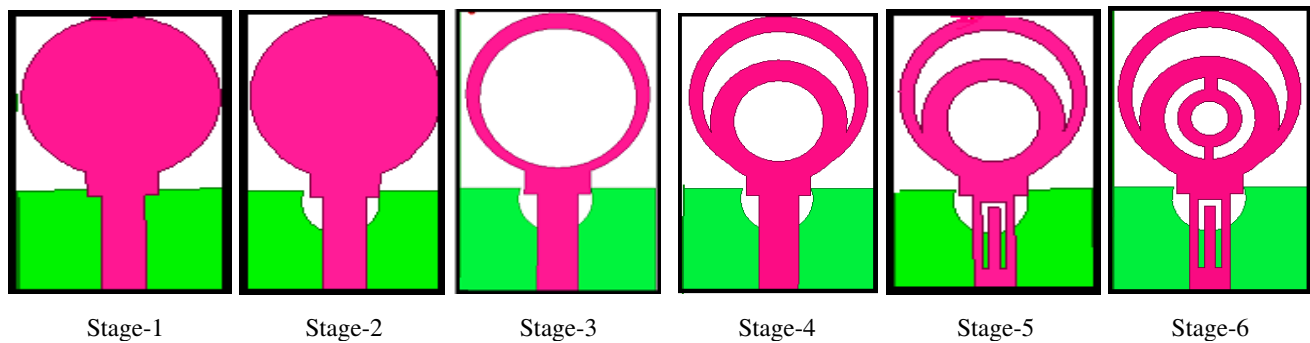


Figure 2. Evolution of the proposed antenna structure at various progressive stages.

Stage-3: In addition to stage-2, the radiator comprises a circular ring which is formed by etching a circular slot. This ring has an outer radius of $R1$ and an inner radius of $R2$. In this stage, the antenna provides band notch at 6–9 GHz. This slot prevents the propagation of electromagnetic surface waves within any specific frequency band which is called as bandgap thus allowing further control of the behavior of electromagnetic waves compared to any guiding which is conventional or any filter structure.

Stage-4: As the intended band notch is at 5.4 GHz and 7.6 GHz, stage 3 is modified as stage 4. It comprises two symmetric rings named as Ring 1 and Ring 2. The outer radius of Ring 1 is $R1$, and inner radius is $R2$. The outer radius of Ring 2 is $R3$, and inner radius is $R4$. There exists a crescent shape slotted structure between Ring 1 and Ring 2. This provides a notch at 5.4 GHz with an elimination of 900 MHz bandwidth ranging from 5.15 to 5.85 GHz.

Stage-5: As stage-4 provides a single band notch at 5.4 GHz and still another band notch is intended, stage-4 is modified as stage-5. It comprises two circular rings named as Ring 1 and Ring 2. A reversed

U-shaped slot is carved on a feeding microstrip line. This provides a notch at 7.6 GHz with the notch bandwidth of 1 GHz ranging from 7 to 8.15 GHz while operating from 3.5 GHz to 12 GHz.

Stage-6: The two intended notches are achieved at stage-5. As an extension of increasing gain ring-3 is inserted. This stage comprises three circular rings named as Ring 1, Ring 2, and Ring 3. The dimensions of Ring 3 are outer radius of $R4$ and inner radius of $R5$. A reversed U-shaped slot is carved on a feeding microstrip line with a defected ground structure. This provides a band notch at 5.4 GHz and 7.6 GHz while operating from 3.5 GHz to 12 GHz, and gain of the antenna is improved which is depicted in Figure 5.

The extent of the slot is around $\frac{\lambda}{2}$ at the center frequency of band that is to be notched which is calculated by the following formulae (1), (2), (3) [13]:

$$\frac{LL_o + LL_i}{2} = \frac{c}{2f_{\text{center}}\sqrt{\varepsilon_{\text{eff}}}} \quad (1)$$

$$\varepsilon_{\text{eff}} = \frac{\varepsilon_{r+1}}{2} \quad (2)$$

c is the light speed;

f_{center} is the center frequency of band that is to be notched;

ε_r represents the relative permittivity;

ε_{eff} represents the effective dielectric constant;

where LL_o is the length of outer arc of the crescent slot that is etched. It is calculated by using the following equation

$$LL_o = 2(\pi - \arccos((h_1 + d_2)/R_2)) R_2 \quad (3)$$

$h_1, d_1 = |O1 - O2|, d_2 = |O2 - O3|$, $O1$ is the center of outer circle of Ring-1, $O2$ the center of inner circle of Ring-1, $O3$ the center of outer circle of Ring-2, and R_2 are the geometric meanings of parameters shown in Figure 1. The value π & $\arccos((h_1 + d_2)/R_2)$ are in radians.

LL_i is the length of inner arc of the crescent slot that is calculated by using the following equation

$$LL_i = 2(\pi - \arccos h_1/R_3) R_3 \quad (4)$$

where h_1 and R_3 are geometric parameters, and the value π and $\arccos(h_1/R_3)$ are in radians.

Length L_s of inverted U slot is calculated by using the equation [14].

$$L_s = \frac{c}{2f_{\text{center}}\sqrt{\varepsilon_{\text{eff}}}} \quad (5)$$

3. PARAMETRIC OPTIMIZATION

The parameter $R2$ for Ring-1 is varied in steps from 5.6 mm to 5.8 mm, and resultant VSWR is observed. The optimized value of $R2 = 5.8$ is chosen. The parameter $R4$ for Ring-2 is varied from 3.2 mm to 3.4 mm. The optimized value for $R4 = 3.4$ mm is chosen. The parameter $R6$ of Ring-3 is varied from 1.2 to 1.4. The optimized value for $R6 = 1.4$ is chosen. The parameter $L4$ of the inverted U shaped slot is varied in steps of 0.1 from 5.2 mm to 5.6 mm, and it is found that the best rejection occurs for the length $L4$ of 5.6 mm. All the optimized values are chosen for providing the desired characteristics. The plots regarding all these optimetrics are depicted in Figures 3(a)–(d).

The comparison of VSWR at different stages is displayed in Figure 4. The comparison of gains at six stages is displayed in Figure 5.

A VSWR of greater than 2 is obtained for the proposed antenna at the dual notched bands which rejects WLAN and X-bands while it is less than 2 for the remaining operating band as displayed in Figure 4. The performance of antenna is excellent over operational bandwidth and has good filter's ability to reject the required frequency. Further, it is compact in size.

Figure 6 illustrates the surface current spreading at the notched bands. Less current distributions at 5.4 GHz and 7.6 GHz are found.

Figure 6 shows the distribution of surface current at different frequencies. It is noticed from Figure 6(a) at 4 GHz and Figure 6(d) at 9 GHz, which are operating frequencies, that surface current is

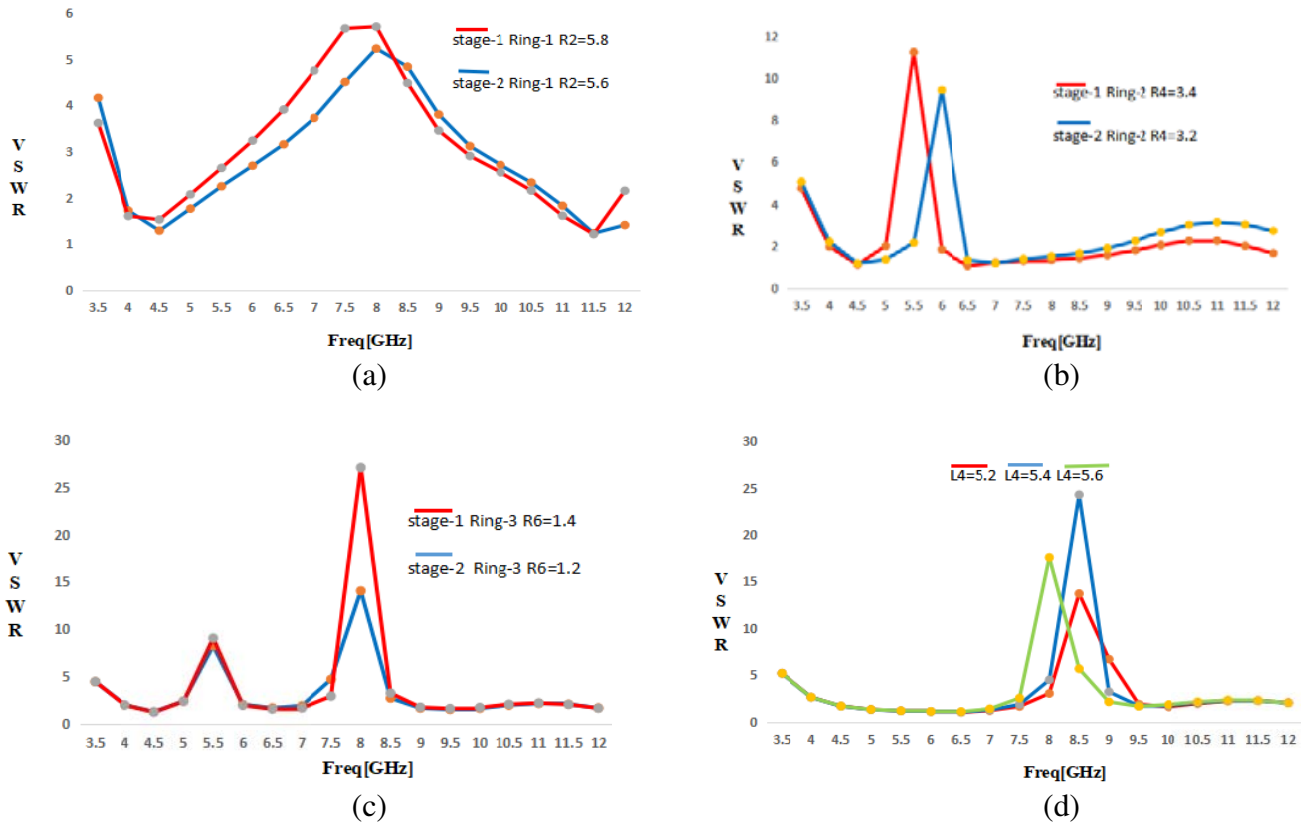


Figure 3. Optimetrics for various parameters.

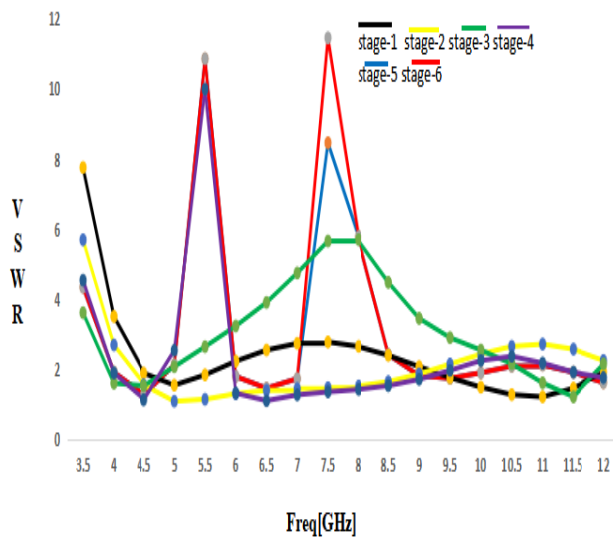


Figure 4. VSWR plots for six stages in the evolution.

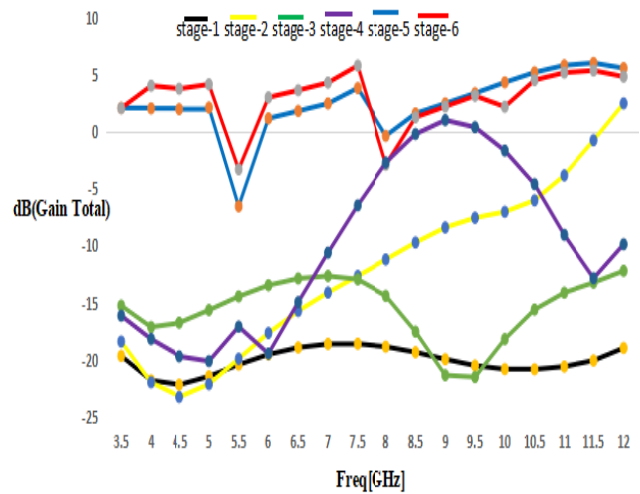


Figure 5. Comparison of gain for six stages in the evolution.

scattered throughout the radiating structure. It is noticed from Figure 6(b) at 5.4 GHz, which is a notch frequency, that the surface current looks intense at the edges of crescent slots because this crescent slot is responsible for obtaining the notch at 5.4 GHz by reducing the overall radiation of the antenna. It is seen from Figure 6(c) that surface current looks intense around the inverted U slot that is accountable for obtaining the notch frequency at 7.6 GHz by reducing the overall radiation of the antenna.

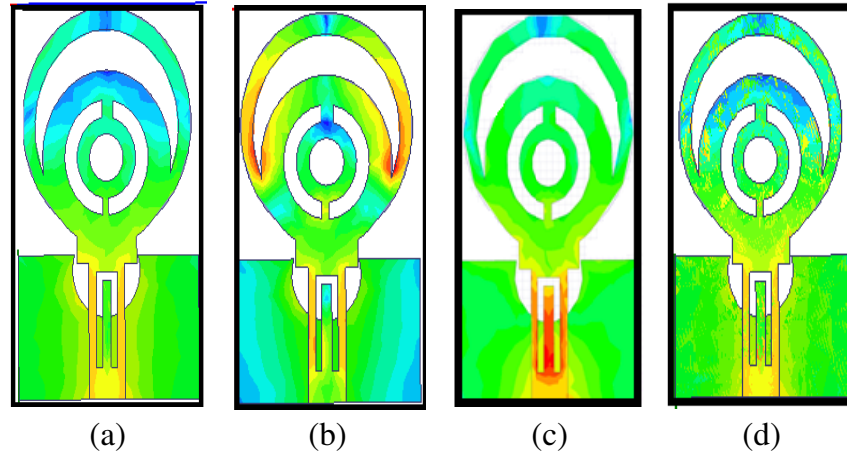


Figure 6. Surface current distribution on single antenna. (a) 4 GHz, (b) 5.4 GHz, (c) 7.6 GHz, (d) 9 GHz.

4. FOUR PORT MIMO ANTENNA DESIGN WITH DUAL NOTCHES

This part emphasizes on the design and investigation of MIMO antenna, with four port, four element achieving dual notches. The dimension of MIMO antenna is $44 \times 44 \times 1.6 \text{ mm}^3$ where $L_m = W_m = 44 \text{ mm}$. The positioning of each element is placed orthogonally to its neighboring element as shown in Figure 7. A great degree of isolation among the elements is realized, without the use of any added circuitry. The alignment of radiating fields is orthogonal with respect to each other, thus minimizing the mutual coupling.

The plot of VSWR and return loss of MIMO antenna is displayed in Figure 9. The MIMO antenna provides an impedance bandwidth of 8.5 GHz ranging from 3.5 to 12 GHz with dual notches at 5.15–5.85 GHz and 7–8.15 GHz. The isolation between the ports is found to be $> 15 \text{ dB}$, and the gain deviates from 5 to 9 dBi over the operating band.

The fabricated prototype is as shown in Figure 8.

All the elements are connected with SMA (Sub Miniature Version A) connectors. For validation, the results are measured by means of vector network analyzer of model N5242A (product by Agilent PNA X series). The simulated and measured VSWRs and return losses at ports 1, 2, 3, 4, i.e., S_{11} , S_{22} , S_{33} , S_{44} , of MIMO antenna are plotted as shown in Figure 9.

There are some disturbances/losses causing slight deviation between simulated and measured values due to soldering material which connects an SMA connector to the feedline and ground of MIMO antenna.

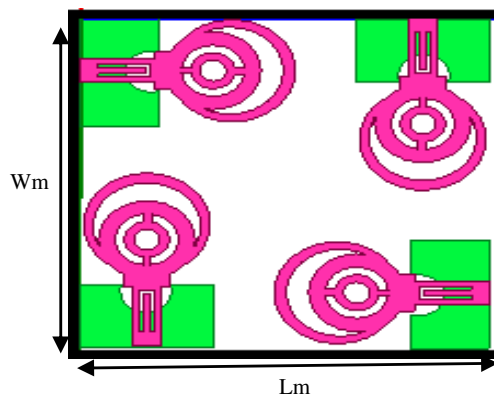


Figure 7. Geometry of the four port MIMO.

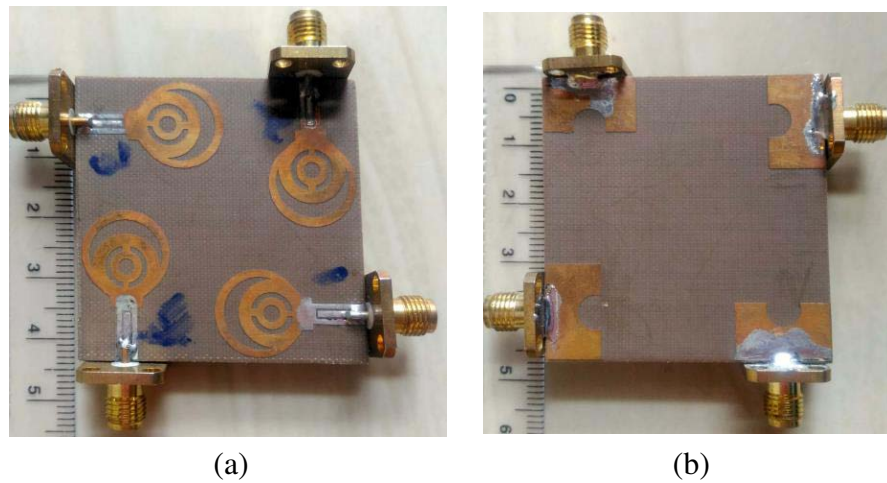


Figure 8. Prototype of MIMO antenna. (a) Top vision and (b) bottom vision.

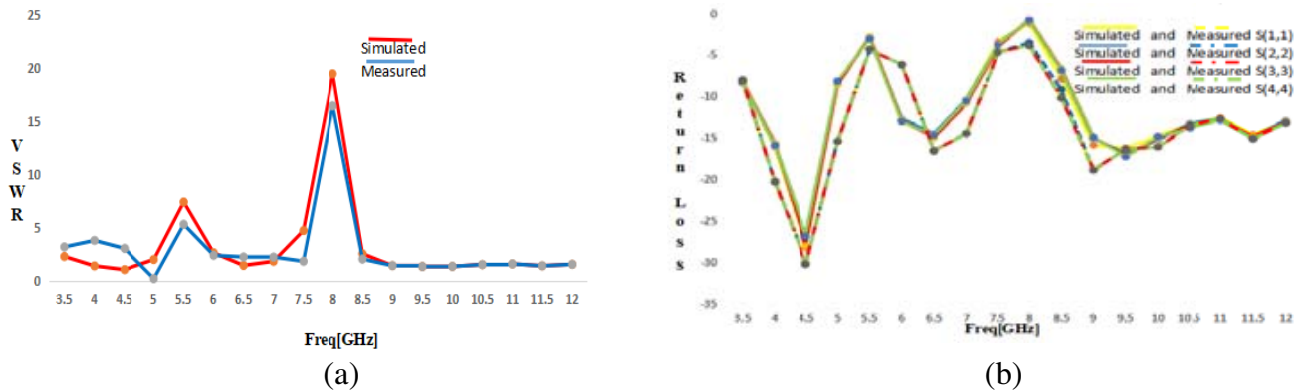


Figure 9. VSWR and return loss plot for dual band notches. (a) Frequency vs VSWR, (b) frequency vs S_{11} , S_{22} , S_{33} , S_{44} .

As illustrated in Figure 9(b), the antenna provides an impedance bandwidth ($|S_{11}| \leq -10$ dB) from 3.5 GHz to 12 GHz except for 5.15–5.85 GHz (WLAN band) and 7–8.15 GHz (X-band for satellite communication). It can be perceived from Figure 10 that the isolation ($|S_{12}|, |S_{13}|, |S_{14}|$) between any two antenna elements is more than 15 dB through the whole working band.

4.1. Radiation Patterns

The E and H -plane patterns at 3.5 GHz, 4.5 GHz, 6.5 GHz, & 10 GHz are plotted as displayed in Figure 11. The simulated CO-POL is shown in Red colour. The simulated CROSS-POL is displayed in Blue colour. The measured CO-POL is shown in Red dots. The measured CROSS-POL is shown in Blue dots.

The 3D polar plots at 3.5 GHz, 4.5 GHz, 6.5 GHz, and 10 GHz are shown in Figure 12.

4.2. Diversity Performance

Envelope correlation coefficient (ECC) characterizes a significant factor that indicates diversity performance of any MIMO antenna. For practical applications, ECC values below 0.1 denote the perfect diversity performance. It is evaluated by means of far field radiation patterns as given by

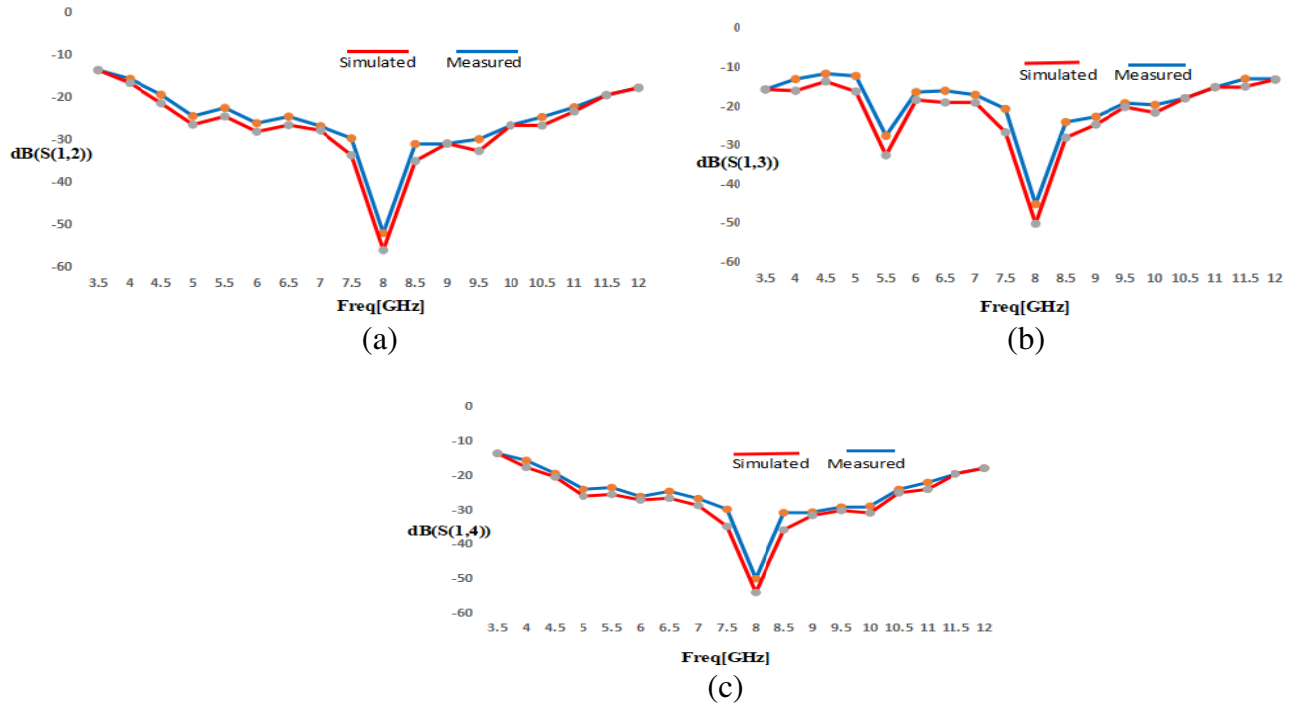


Figure 10. Simulated and measured S -parameters. (a) $|S_{12}|$, (b) $|S_{13}|$, (c) $|S_{14}|$.

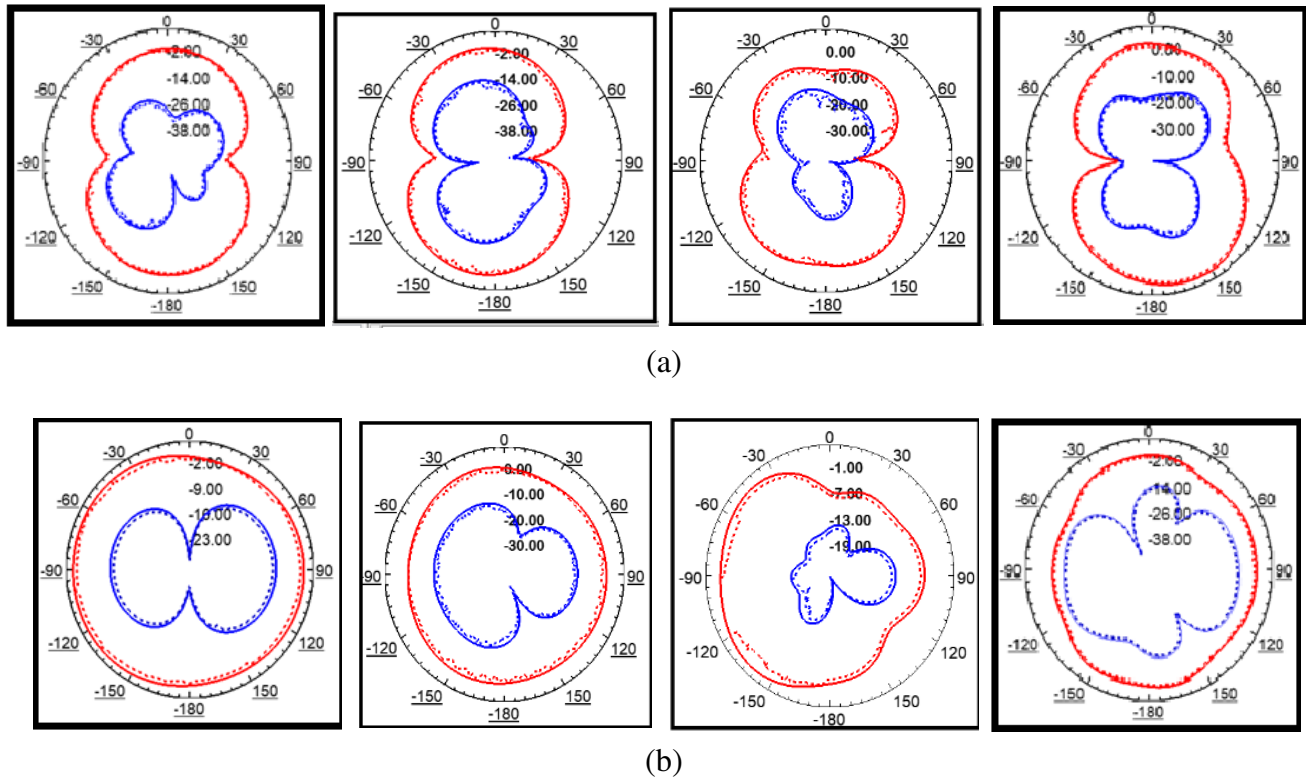


Figure 11. (a) E plane patterns at 3.5 GHz, 4.5 GHz, 6.5 GHz and 10 GHz, (b) H plane patterns 3.5 GHz, 4.5 GHz, 6.5 GHz and 10 GHz.

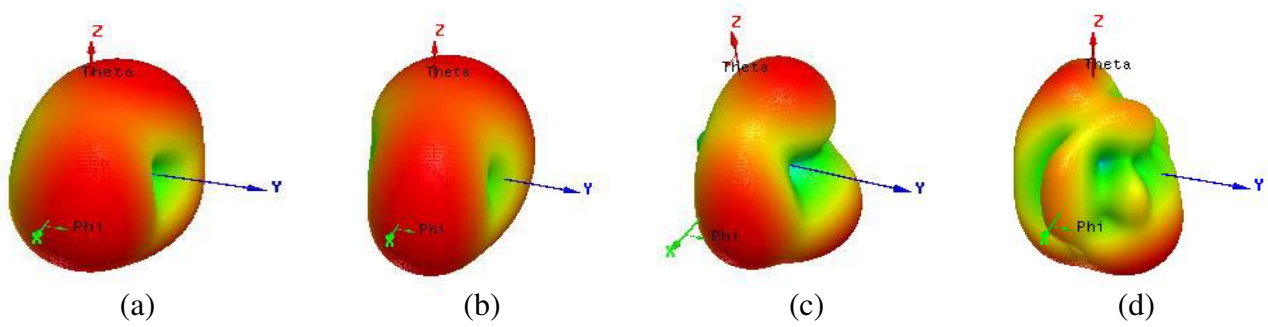


Figure 12. 3D polar plots at 3.5 GHz, 4.5 GHz, 6.5 GHz and 10 GHz.

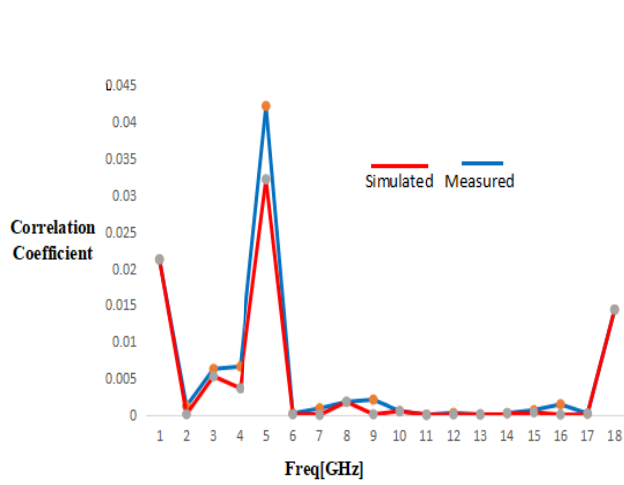


Figure 13. ECC of the MIMO antenna.

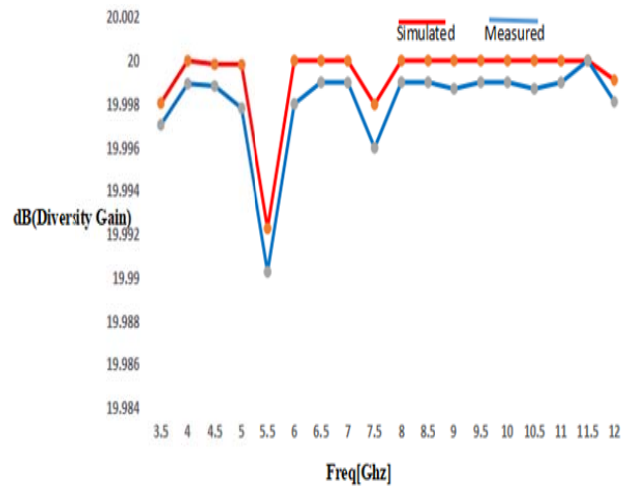


Figure 14. Diversity gain of the MIMO antenna.

Equation (6) [11].

$$\rho_e = \frac{\left| \int_0^{2\pi} \int_0^\pi (XPR \cdot E_{\theta 1} \cdot E_{\theta 2}^* \cdot P_\theta + E_{\varphi 1} \cdot E_{\varphi 2}^* \cdot P_\varphi) d\Omega \right|^2}{\int_0^{2\pi} \int_0^\pi (XPR \cdot E_{\theta 1} \cdot E_{\theta 2}^* \cdot P_\theta + E_{\varphi 1} \cdot E_{\varphi 2}^* \cdot P_\varphi) d\Omega \times \int_0^{2\pi} \int_0^\pi (XPR \cdot E_{\theta 1} \cdot E_{\theta 2}^* \cdot P_\theta + E_{\varphi 1} \cdot E_{\varphi 2}^* \cdot P_\varphi) d\Omega} \quad (6)$$

Figure 13 shows the ECC curves of proposed antenna. It is noticed that ECC values are below 0.05 throughout the operating band from 3.5 GHz to 12 GHz.

The diversity gain of MIMO configuration is evaluated by means of the following equation

$$DG = 10\sqrt{1 - ECC^2} \quad (7)$$

It is plotted in Figure 14.

Total active reflection coefficient (TARC) denotes the square root of the total ratio of reflected power to incident power & the apparent return loss of the entire MIMO antenna. For a dual-port MIMO system, TARC is evaluated by means of the following Equation (8) [12].

$$TARC = \sqrt{\frac{(|S_{11} + S_{12} + S_{13} + S_{14}|^2 + |S_{21} + S_{22} + S_{23} + S_{24}|^2 + |S_{31} + S_{32} + S_{33} + S_{34}|^2 + |S_{41} + S_{42} + S_{43} + S_{44}|^2)}{4}} \quad (8)$$

It is plotted in Figure 15.

Aimed at MIMO communication system, TARC should be < 0 dB. The plot of TARC is shown in Figure 15. It is noticed that its value is < -10 dB in the whole operating band.

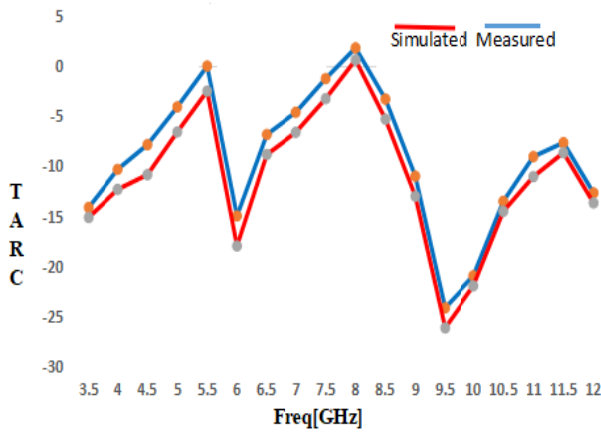


Figure 15. Frequency vs TARC.

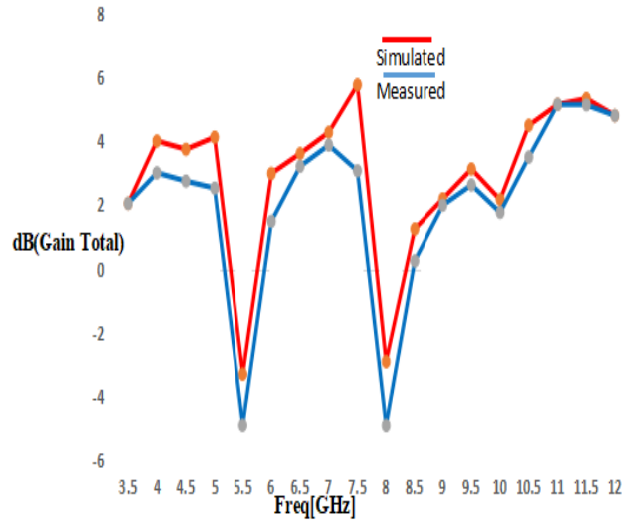


Figure 16. Frequency vs gain.

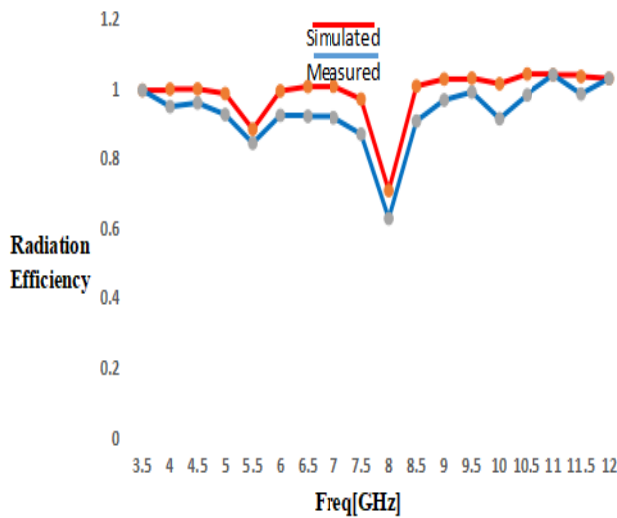


Figure 17. Frequency (GHz) vs radiation efficiency.

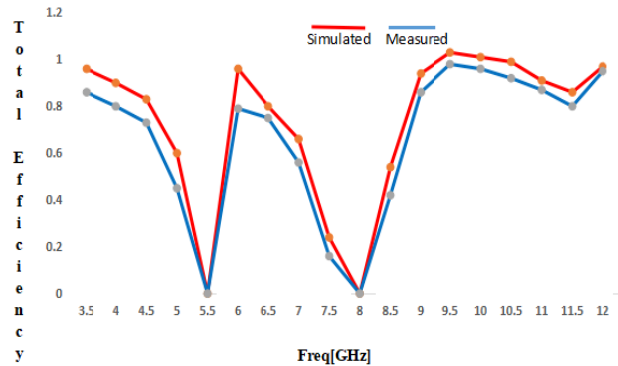


Figure 18. Frequency (GHz) vs total efficiency.

The gain variation is shown in Figure 16. The magnitude of the gain is very low at the center frequency of WLAN and X bands for satellite communication as the antenna is aimed for band rejection at these frequencies. It can be found that the gain of the antenna is greater than 4 dB in the non-notched band. In the notch band, the antenna gain decreases sharply and is less than -6 dB, which indicates that antenna has better band-notched characteristics.

The plot of radiation efficiency is displayed in Figure 17. It can be understood that the radiation efficiency is 95%.

The total efficiency of MIMO antenna is calculated from the following formula [15]

$$\text{Total Efficiency} = (1 - |\text{TARC}|^2) * \text{Radiation efficiency} \tag{9}$$

The corresponding total efficiency plot is displayed in Figure 18.

The plot of group delay is shown in Figure 19. It lies in between 0.80–1 ns.

Table 2. Comparison of dimension of antenna cited in the references.

| Reference | Size in terms of wavelength | Material | Impedance bandwidth (GHz) | Notched band (GHz) | Isolation (dB) | ECC |
|-----------------|--|-----------------------|---------------------------|------------------------------|----------------|------------------|
| [5] | $0.84\lambda \times 0.89\lambda \times 0.016\lambda$ | FR4 | (3.1–11.4 GHz) | 4.8 GHz & 7.7 GHz | > 18 | < 0.1 |
| [9] | $0.57\lambda \times 0.57\lambda \times 0.007\lambda$ | FR4 | 2.8–13.3 | 3.5 GHz & 5.5 GHz | > 19 | < 0.03 |
| [7] | $0.87\lambda \times 0.87\lambda \times 0.026\lambda$ | FR4 | 5–40 GHz | 3.5 GHz & 5.5 GHz | > 18 | < 0.002 |
| [10] | $0.33\lambda \times 0.33\lambda \times 0.016\lambda$ | Rogers 5880 substrate | 2–12 GHz | 3.5 GHz & 5.5 GHz | - | < 0.12 |
| Proposed | $0.51\lambda \times 0.51\lambda \times 0.018\lambda$ | ARLON (AD430) | 3.5–12 GHz | 5.4 GHz & 7.8 GHz | > 15 | < 0.05 |

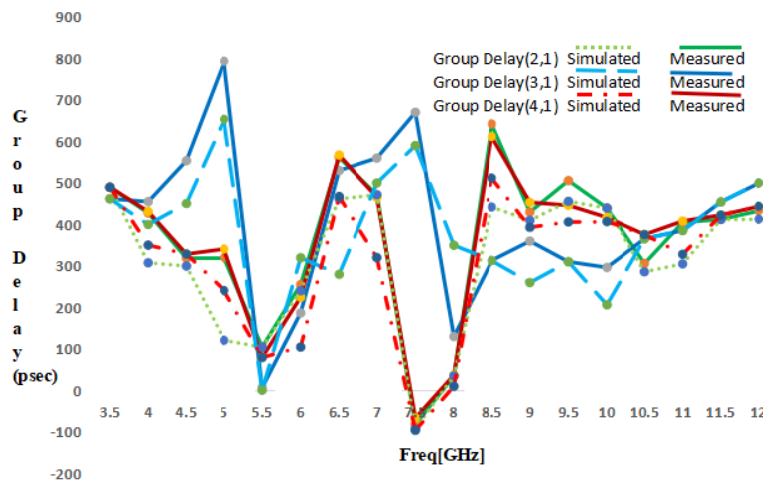


Figure 19. Frequency (GHz) vs group-delay (psec).

Table 2 discusses the comparison of available literature with the proposed antenna in terms of dimensions, material, notched bands, and isolation.

It is found that the proposed antenna is of compact size with sufficient isolation.

5. CONCLUSION

In this paper, a very compact planar MIMO antenna which provides dual notches at WLAN & X-bands for satellite communication is analyzed and designed. Circular rings and slotted microstrip feeding lines play a main role in achieving desired band notches. The modified defected ground plane is a rectangular structure with a semicircle slot at its center which is used to obtain broad impedance bandwidth. The proposed MIMO antenna with acceptable performance in ECC, diversity gain, TARC, radiation efficiency, and group delay is achieved. As of its compact size, it is very much suitable for portable IOT applications.

REFERENCES

1. Hossain, E. and V. K. Bhargava, *Cognitive Wireless Communication Networks*, Springer Science and Business Media, LLC, 2007.
2. Federal Communications Commission, First Report and Order, “Revision of Part 15 of the Commission’s rule regarding UWB transmission system,” FCC 02-48, 2002.

3. Allen, B., *UWB Antennas and Propagation for Communications, Radar and Imaging*, Wiley, 2006.
4. Zhao, Y., F.-S. Zhang, L.-X. Cao, and D.-H. Li, "A compact dual band-notched MIMO diversity antenna for UWB wireless applications," *Progress In Electromagnetics Research C*, Vol. 89, 161–169, 2019.
5. Srivastava, K., A. Kumar, B. K. Kanaujia, S. Dwari, and S. Kumar, "A CPW-fed UWB MIMO antenna with integrated GSM band and dual band notches," *International Journal of RF and Microwave Computer-Aided Engineering*, 2019.
6. Zhang, J., L. Wang, and W. Zhang, "A novel dual band-notched CPW-fed UWB MIMO antenna with mutual coupling reduction characteristics," *Progress In Electromagnetics Research Letters*, Vol. 90, 21–28, 2020.
7. Raheja, D. K., S. Kumar, and B. K. Kanaujia, "Compact quasi elliptical self complementary four port super wideband MIMO antenna with dual band elimination characteristics," *International Journal of Electronics and Communications (AEÜ)*, Vol. 114, 153001, 2020.
8. Srivastava, G., L. H. Son, R. Kumar, and M. Khari, "A dual band notched ultra-wideband antenna," *Wireless Personal Communications*, Vol. 110, No. 1, 2019.
9. Kumar, S., G. H. Lee, D. H. Kim, W. Mohyuddin, H. C. Choi, and K. W. Kim, "Multiple-input-multiple-output/diversity antenna with dual band-notched characteristics for ultrawideband applications," *Microwave and Optical Technology Letters*, 2019.
10. Liu, H., G. Kang, and S. Jiang, "Compact dual band-notched UWB multiple input multiple-output antenna for portable applications," *Microwave and Optical Technology Letters*, Vol. 62, No. 4, 2020.
11. Knudsen, M. B. and G. F. Pedersen, "Spherical outdoor to indoor power spectrum model at the mobile terminal," *IEEE J. Sel. Areas Commun.*, Vol. 20, 1156–1168, 2002.
12. Khan, M. S., A. Iftikhar, R. M. Shubair Antonio-Daniele Capobianco, S. M. Asif, B. D. Braaten, and D. E. Anagnostou, "Ultra-compact reconfigurable band reject UWB MIMO antenna with four radiators," *Electronics*, Vol. 9, No. 4, 584, 2020.
13. Wu, W., B. Yuan, and A. Wu, "A quad-element UWB-MIMO antenna with band-notch and reduced mutual coupling based on EBG structures," *International Journal of Antennas and Propagation*, Vol. 2018, 10 pages, 2018.
14. Sohail, A., K. S. Alimgeer, A. Iftikhar, B. Ijaz, K. W. Kim, and W. Mohyuddin, "Dual notch band UWB antenna with improved notch characteristics," *Microwave and Optical Technology Letters*, Vol. 60, No. 4, 2018.
15. Wang, M., T.-H. Loh, Y. Zhao, and Q. Xu, "A closed-form formula of radiation and total efficiency for lossy multiport antennas," *IEEE Antennas and Wireless Propagation Letters*, Vol. 18, No. 12, 2468–2472, 2019.